CSI TECHNOLOGY VALIDATION ON AN LSS GROUND EXPERIMENT FACILITY

S. J. Wang
D. B. Eldred
Jet Propulsion Laboratory
California Institute of Technology
Pasadena, California

The Third NASA/DOD CSI Conference
January 30 - February 2, 1989
San Diego, California

Flexible Spacecraft Control Dynamics
Simulator Development

For the last 10 years, JPL has been actively engaged in the development of new technologies for the identification and control of large flexible space structural systems. The objectives have been developing both new concepts, theories, and hardware, as well as to extend state-of-the-art methodologies to a breadboard level of maturity for in flight applications. To accomplish this, technology validation through experimental demonstration on a real physical structure becomes necessary.

Recognizing this need, JPL, under the joint sponsorship of the Air Force Astronautics Laboratory (AFAL) and NASA Office of Aeronautics and Space Technology (NASA/OAST), has developed a large ground structure test bed called: Flexible Spacecraft Control Dynamics Simulator.

The experiment structure, which is best described as resembling a large space antenna, was designed to possess generic LSS properties, particularly multiple, densely packed, lightly damped vibration modes. Multiple sensors and actuators are distributed throughout the structure, and a microcomputer workstation and a data acquisition system, together with an advanced programming environment (implemented in Ada), facilitate control experiments on the Simulator system.

- **OBJECTIVE**
  - DEMONSTRATE AND EVALUATE NEW, EVOLVING AND CRITICAL CONTROL METHODOLOGIES ON A REALISTIC LARGE FLEXIBLE STRUCTURE WITH PRACTICAL HARDWARE AND COMPUTATIONAL RESTRICTIONS
- **EXPERIMENT STRUCTURE**
  - RESEMBLES A LARGE ANTENNA
  - 40 MODES BELOW 5 Hz
  - 30 SENSORS AND 14 ACTUATORS
  - MICROCOMPUTER WORKSTATION CONTROL AND COMPUTERIZED DATA ACQUISITION SYSTEM
  - ADVANCED PROGRAMMING ENVIRONMENT
- **TARGET METHODOLOGIES FOR EVALUATION**
  - ADAPTIVE AND RECONFIGURABLE CONTROL
  - ROBUST AND DISTRIBUTED CONTROL
  - SYSTEM PARAMETER IDENTIFICATION
  - SHAPE DETERMINATION AND CONTROL
  - ADVANCED OPTICAL SENSING TECHNOLOGY

Experiment Structure

Figure 1 shows a schematic overview of the experiment structure. The main components of the structure consist of 12 ribs, the central hub, the flexible boom, and the feed mass. The overall diameter of the structure is 18.5 feet. Each of the steel ribs is supported at two locations by zero-stiffness "levitators" in order to prevent excessive sag due to gravity. A levitator consists of a counterweight hanging over a low friction pulley. This suspension design provides a nearly constant supporting force throughout a large range of motion. The ribs are each rigidly attached to the central hub which consists of three concentric rings constructed from tubular steel. The inner ring is rigidly mounted to the backup structure via a bipod arrangement. The center ring is attached to the inner ring via two flexure bearings, and it rotates about an axis which lies in the horizontal plane. The outer ring, which contains the rib mounting pads, is attached to the center ring via two more flexures.

The three rings together comprise a gimbal mounting arrangement. A flexible boom hangs downward, and a 10 pound weight hangs from its lowest point, simulating the feed and flexible feed boom of a large flexible antenna.

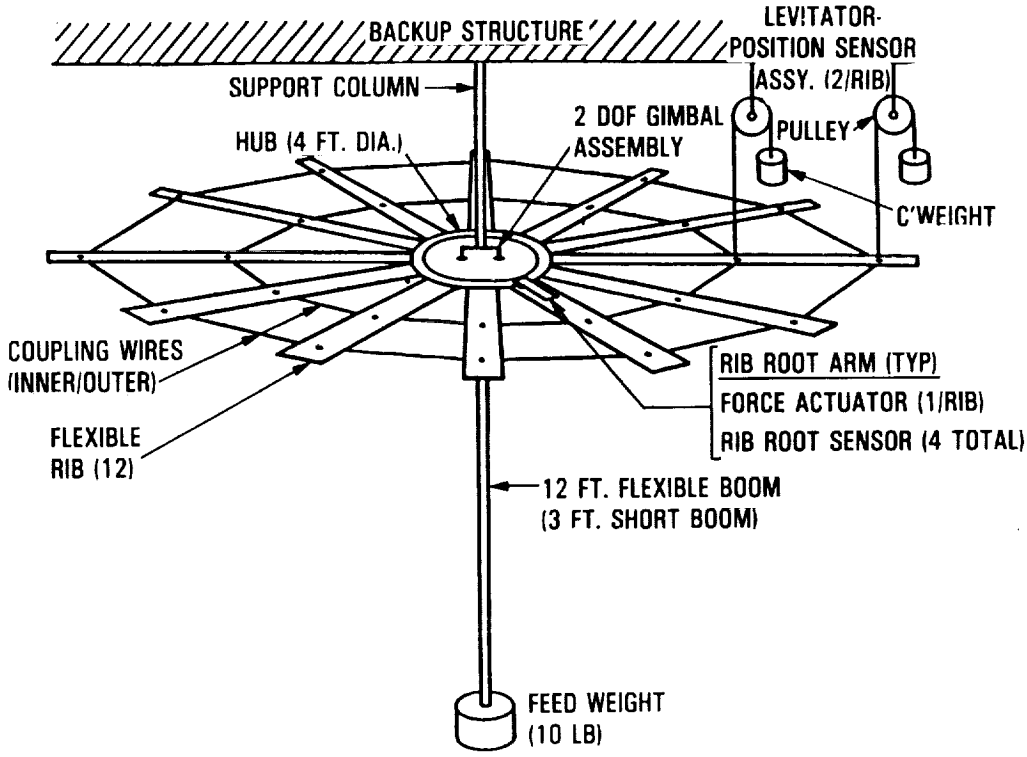

Figure 1.

Figure 2 shows a photograph of the experiment structure and supporting hardware. The 12 ribs and the gimbal-hub are painted white for visibility. The rib-to-rib coupling is provided by the two rings of pretensioned steel wires which can be identified by the tapes attached to them. Above the experiment structure is a backup structure which provides precision mounting for the levitators and for the hub gimbal bearings, and hence, for the entire experiment structure. The supporting structure is constructed of truss members and tension cables, and its lowest vibration frequency is 15 Hz; this high stiffness is sufficient to prevent interaction with the experiment structure.

The cables extending upward from the top of the backup structure allow the entire structure to be raised to the 20-foot level to allow for sharing of the laboratory with other programs.

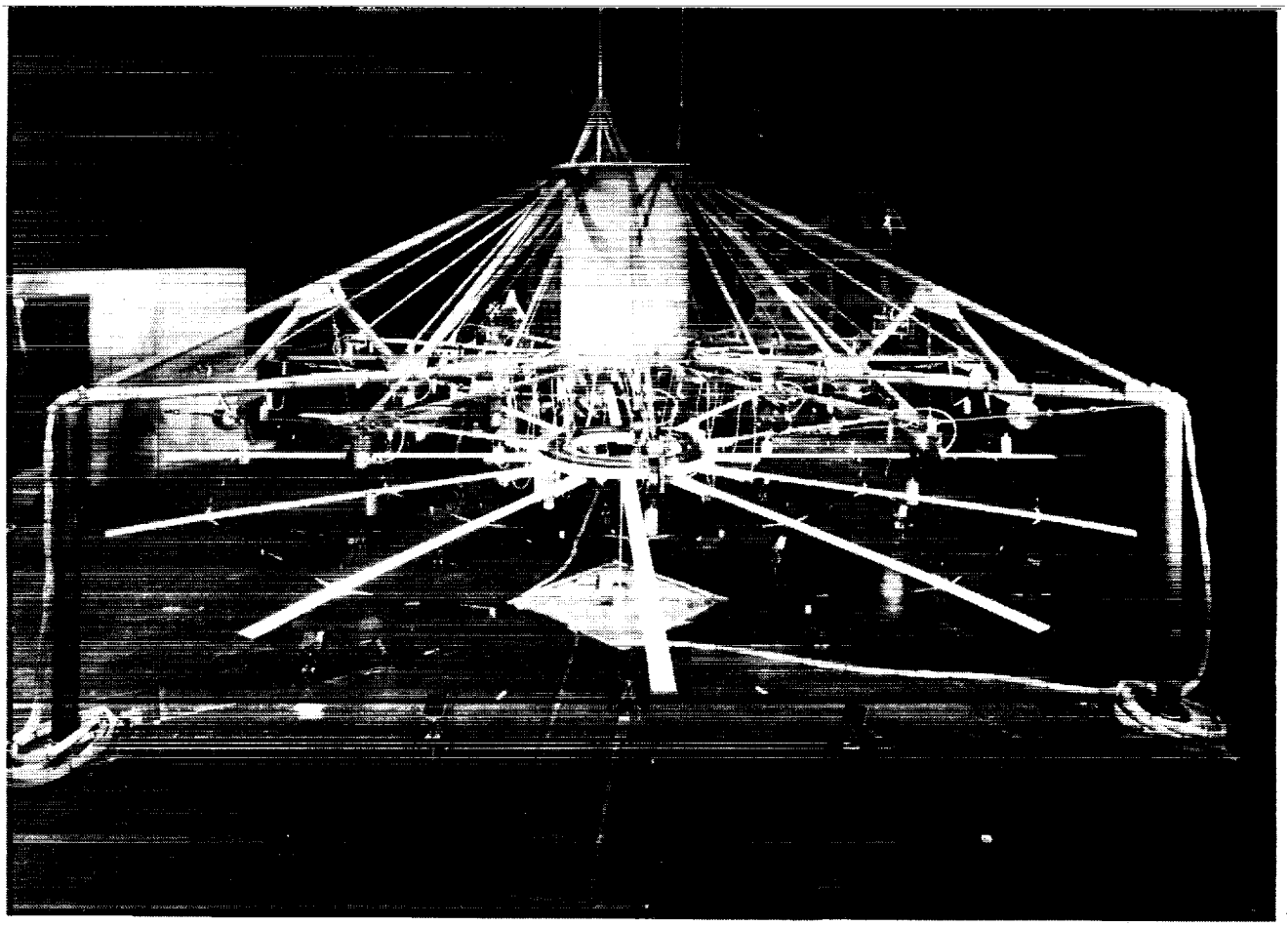

Figure 2.

Transducer Locations

Sensing instrumentation includes 24 levitator sensors, 4 rib-root sensors, and 2 hub-angle sensors, whose locations are shown in Figure 3. The levitator sensors consist of optical incremental encoders which are integrated with the levitator pulleys and measure pulley rotation. The rib root sensors employ LVDT's (linear variable differential transformer) to measure rib displacement at locations near their attachments to the hub, relative to brackets attached rigidly to the hub. The hub angle sensors are RVDT's (rotory variable differential transformer) which are mounted coaxial with the hub gimbal bearings and thus measure hub rotation about its two gimbal axes.

Actuation includes 12 rib-root actuators and 2 hub torquers. The rib-root actuators consist of linear voice-coil devices which react between the ribs and the rib-root sensor brackets. They are mounted close to the rib-root sensors to provide essentially collocated sensing and actuatuation. The hub torquers are non-contacting linear motors which react between the hub and the backup structure, thereby applying torques to the hub. These actuators use a flat air-core armature coil which passes between the poles of a larger permanent magnet.

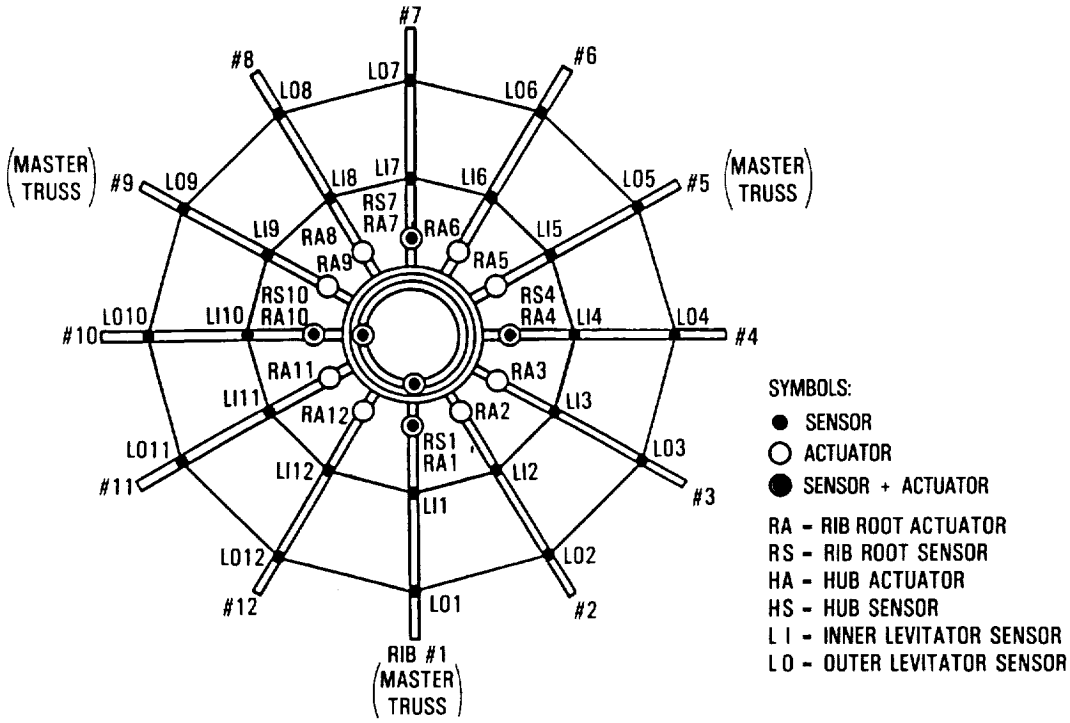

Figure 3.

Normal Modes

The following tables show the vibration modes of the experiment structure with higher modes (above 10 Hz) truncated from the lists. The modes are divided into two groups: the boom-dish modes and the dish modes. The former are the anti-symmetric modes about the central hub, and the later are the symmetrical ones. The distinguishing property of the antisymmetric modes is that these modes include rotation of the gimballed hub, whereas the hub remains stationary for all the symmetric modes. Table I shows the boom-dish modes when the short boom, 3 feet in length, is used, whereas Table II shows those corresponding to the long boom which is 12 feet long. As designed, the modes are densely packed with the lowest modal frequencies of 0.91 Hz and 0.112 Hz depending on what boom is attached to the system. There are 39 modes below 5 Hz in the system with the short boom, and 41 with the long boom arrangement. Dish modes are shown in Table III.

I. BOOM-DISH MODES
(SHORT BOOM CONFIG)

FREQUENCY (HZ)	PIVOT AXIS
0.091	4-10
0.091	1-7
0.616	4-10
0.628	1-7
1.685	4-10
1.687	1-7
2.577	4-10
2.682	1-7
4.858	4-10
4.897	1-7
9.822	4-10
9.892	1-7

II. BOOM-DISH MODES
(LONG BOOM CONFIG)

FREQUENCY(HZ)	PIVOT AXIS
0.112	4-10
0.113	1-7
0.332	4-10
0.332	1-7
0.758	4-10
0.774	1-7
2.264	4-10
2.354	1-7
4.724	4-10
4.726	1-7
4.926	4-10
4.967	1-7

III. DISH MODES (40)

FREQUENCY(HZ)	WAVE NUMBER	FREQUENCY(HZ)	WAVE NUMBER
0.210	0	4.656	0
0.253	2	4.658	2
0.253	2	4.658	2
0.298	3	4.660	3
0.298	3	4.660	3
0.322	4	4.661	4
0.322	4	4.661	4
0.344	5	4.662	5
0.344	5	4.662	5
0.351	6	4.663	6
1.517	0	9.474	0
1.533	2	9.474	2
1.533	2	9.474	2
1.550	3	9.474	3
1.550	3	9.474	3
1.566	4	9.474	4
1.566	4	9.474	4
1.578	5	9.475	5
1.578	5	9.475	5
1.583	6	9.475	6

Tables 1 – 3.

Model Characteristics

Figure 4 shows the plots of the first 12 lowest frequency mode shapes for this system with the short boom which is most commonly used in the experiments. The first (0.09 Hz) and the eighth (0.616 Hz) modes are boom-dish modes and the remainder are dish modes. Due to the symmetry of the structure, many of the modes come in degenerate pairs in that they have virtually identical frequencies and their mode shapes differ only by a phase angle. For higher frequency dish modes, these mode shapes become very close to linear combinations of contilevered rib modes, reflecting the reduced role that its coupling wires play in forming the mode shapes for higher frequency.

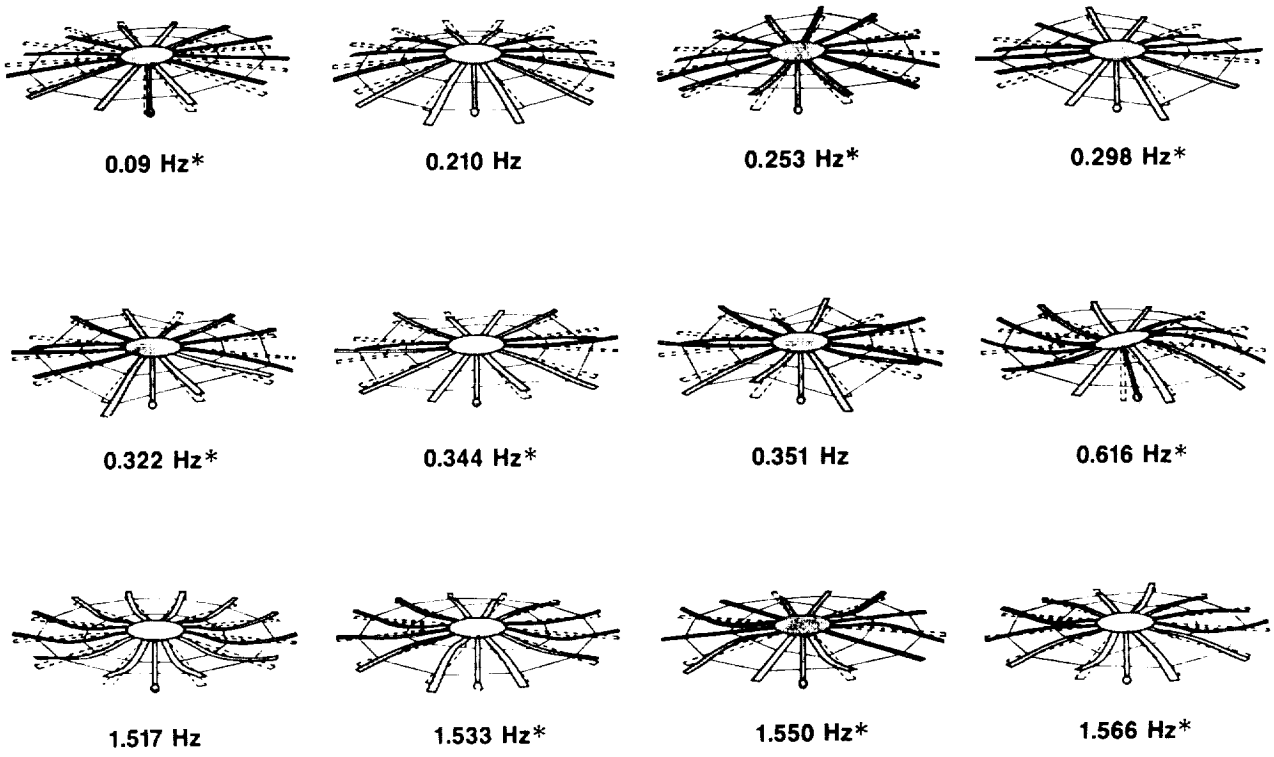

Figure 4.

Adaptive Transient/Deflection Regulation Experiment
(C. Ih, A. Ahmed, D. Bayard, S. Wang)

The objective of adaptive control technology research at JPL is to develop a subsystem adaptive control capability for future space mission applications. The overall approach involves a multilevel adaptation methodology in which a learning and decision making system is employed for high-level controller tuning and a servo level controller is used for adaptation to local properties such as drifting parameters, model uncertainties, and environmental disturbances. The purpose of these experiments is to validate the adaptive control technology on a physical flexible structure system and to demonstrate the controller's effectiveness and performance subject to large model parameter uncertainties, unmodeled dynamics, measurement noise, and dynamic disturbances.

The results of two phases of experiments are discussed here. The Phase I experiments employed two hub sensors and two hub actuators. The Phase II experiments used 6 sensors and 6 actuators consisting of 2 hub sensor and actuator pairs and 4 rib-root sensor and actuator pairs. (Fig. 5.)

OBJECTIVE

TO VALIDATE ADAPTIVE CONTROL TECHNOLOGY FOR UNCERTAINTY MANAGEMENT OF FLEXIBLE SPACE STRUCTURAL SYSTEMS

TO DEMONSTRATE THE EFFECTIVENESS OF ADAPTIVE CONTROL TECHNIQUES FOR TRANSIENT/DEFLECTION REGULATION ON A PHYSICAL PLANT

EXPERIMENT DESIGN

- **SENSORS:** • 2-AXIS HUB ANGLE SENSORS FOR CONTROL • 24 LEVITATION DISPLACEMENT SENSORS FOR MONITORING
- **ACTUATORS:** • 2-AXIS HUB TORQUERS
- **PLANT:** • INFINITE DIMENSIONAL AND LIGHT DAMPING
- **REF. MODEL:** • 2 MODES, HIGH DAMPING, AND LARGE PARAMETER UNCERTAINTIES (50-100%)
- **TRANSIENT REGULATION EXPERIMENT:**
  - REFERENCE MODEL AT QUIESCENT STATE
  - STRUCTURE EXCITATION USING HUB TORQUERS
  - ADAPTIVE CONTROLLER TO FORCE PLANT TO TRACK MODEL FOR VIBRATION SUPRESSION
- **DEFLECTION REGULATION EXPERIMENT:**
  - MANUALLY DEFLECT STRUCTURE
  - MODEL INITIALIZED TO APPROXIMATE STRUCTURE DEFLECTION
  - CONTROLLER TO FORCE PLANT OUTPUT TO TRACK MODEL OUTPUT
- **SAMPLING RATE:** • 20 Hz

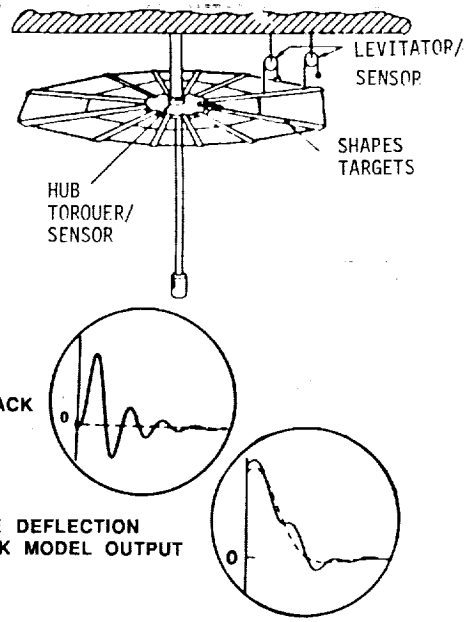

Figure 5.

Adaptive Control System

Figure 6 highlights the model reference adaptive control system concept implemented for the experiments. The system consists of a reference model, the plant, and the adaptive controller. The model is selected based on the knowledge of the plant and the desired performance of the system, and in general, is a low order and high damping system. The model is driven by u_m and its output is y_m. The output error e_y is formulated by comparing the model output with the noise corrupted plant output. The error signal is split into two paths: one fed to the branch filter and the other to the controller directly. Inside the controller, these signals along with the model inputs and states are pre- and post- multiplied by weighting matrices and then they are fed through SPR (strictly positive real) adaptive "filters" where the leakage terms are introduced for gain "retardation." Two sets of adaptive gains are generated: the integral gain K_I and the proportional gain K_P. The control signal u_p is generated by multiplying the gains by the filtered long vector $\bar{r}$.

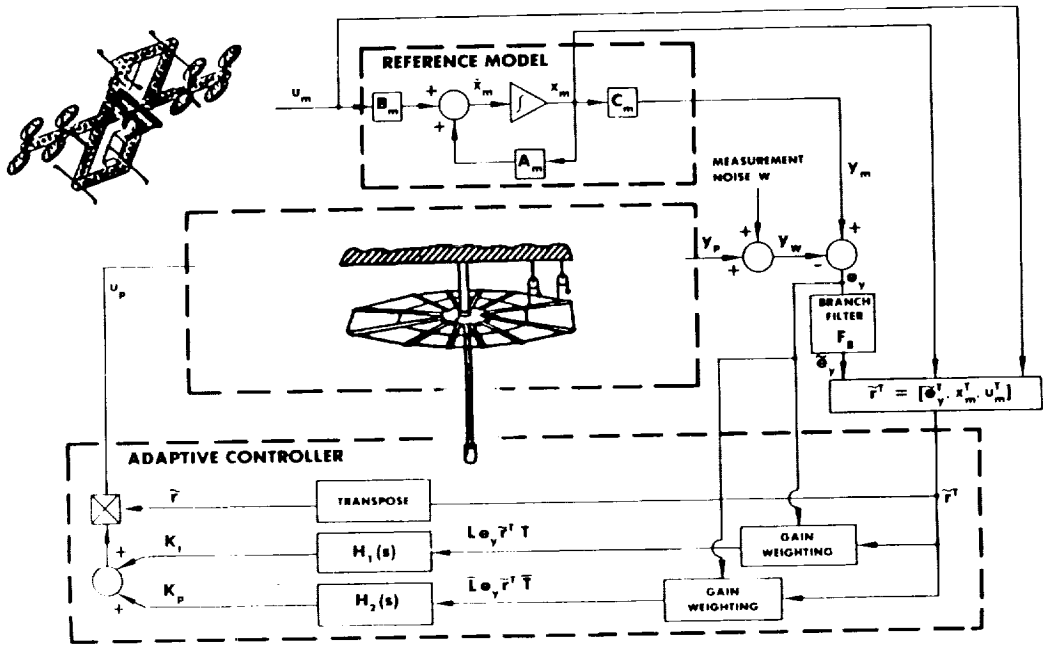

- INNER-LOOP CONTROLLER TO STABILIZE RIGID BODY DYNAMICS
- INPUT GAIN WEIGHTING (L, $\bar{L}$) TO SPATIALLY DISTRIBUTE CONTROL EFFORT FOR REALIZING MULTI-OBJECTIVE DESIGN TRADES
- BRANCH FILTER/SPR ADAPTATION (F_B, $H_1(S)$, $H_2(S)$) TO COMPENSATE FOR DESTABILIZING EFFECT OF MEASUREMENT NOISE

Figure 6.

Adaptive Control Experiment I --
Transient/Deflection Regulation with Hub Sensing/Actuation

The left two plots show the results of the transient regulation experiment. The experiment structure was excited for 2 seconds. The free response shows at least two hub modes were excited: the 0.091 Hz and the 0.616 Hz. The results show a 4.5 to 1 improvement was achieved by the adaptive controller even with 50% - 100% uncertainty of the system parameters was assumed for the controller design. The other two plots show the results of the deflection regulation experiment. The data show that the plant followed the model very well with the transient damped out quickly. A 5.8 to 1 settling time reduction was observed. The controller is robust with high stability margin. (Fig. 7.)

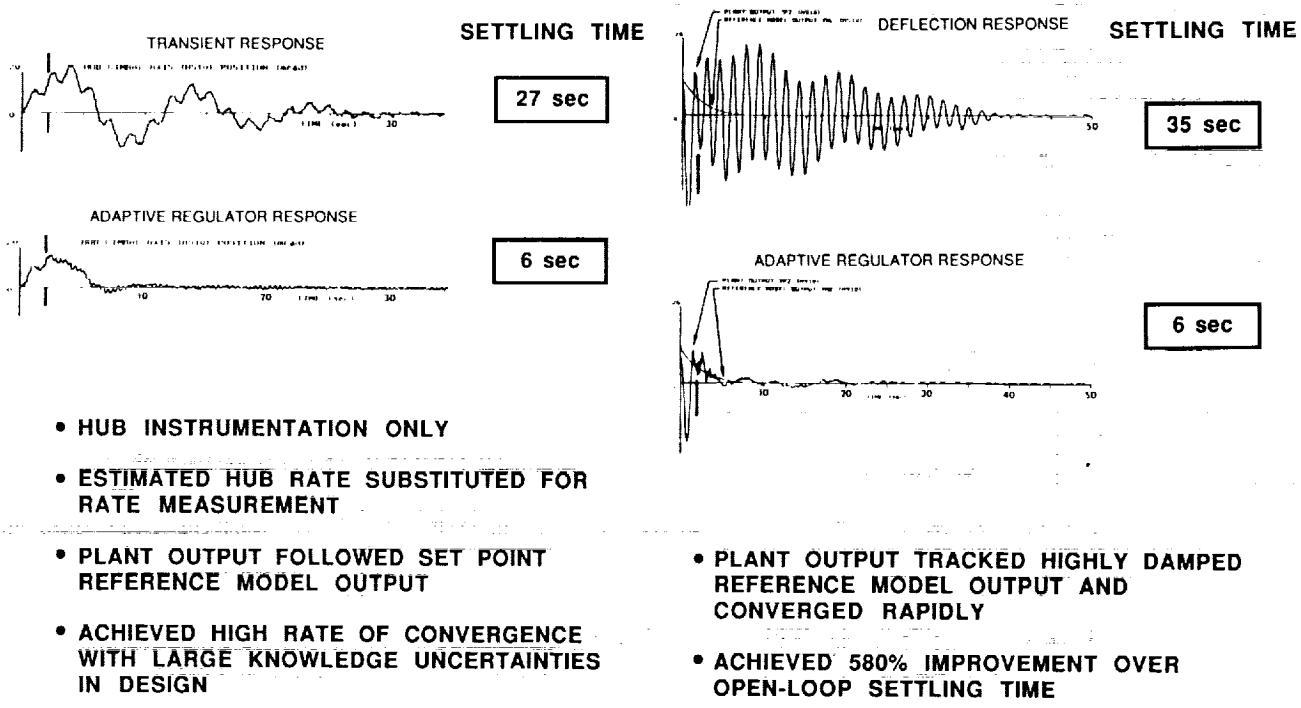

Figure 7.

Adaptive Control Experiment II --
Transient Regulation with Hub and Rib Sensing/Actuation

This experiment demonstrated the adaptive controller's performance for 6 inputs and 6 outputs (2 hub sensor/actuator pairs and 4 rib-root sensor/actuator pairs), again with high model uncertainties and truncation of unmodelled dynamics. The controller controls both boom-dish modes and dish modes. Because the sensor output is position and not rate, rates were estimated using a 24-state Kalman filter; this along with the computing hardware limitations has severely impacted on the performance of the controller. Even with these constraints, high performance has been achieved by the adaptive controller. (Fig. 8.)

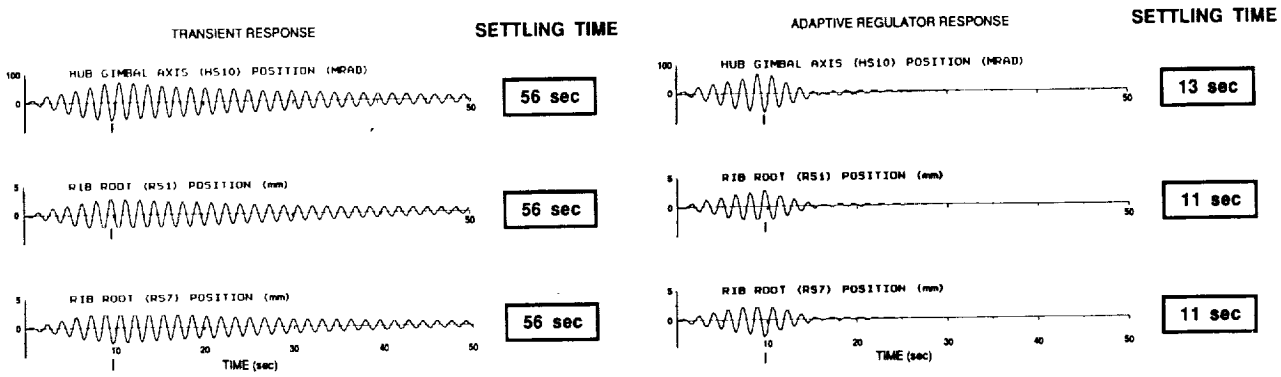

- 6 INPUTS (2 HUB TORQUERS AND 4 RIB-ROOT ACTUATORS) AND 6 OUTPUTS (2 HUB ANGLE SENSORS AND 4 RIB-ROOT DISPLACEMENT SENSORS)
- ESTIMATED HUB AND RIB-ROOT RATES
- ACHIEVED HIGH PERFORMANCE WITH LARGE KNOWLEDGE UNCERTAINTIES IN DESIGN

Figure 8.

Vibration Damping and Robust Control
of Flexible Space Structure
Using μ-Synthesis Techniques
(G. Balas, C. Chu, J. Doyle)

This research employs μ-based control design methods for the analysis and synthesis of controllers for lightly damped flexible structures. The Flexible Spacecraft Control Dynamics Simulator provides a test bed for validation of this methodology and for exploration of critical robust control design issues.

The results discussed here (Experiment I) deal primarily with the design of a high performance vibration attenuation controller for the simulator using only the hub actuators and sensors and employing a design model with the first two global flexible modes. For robust control design, the effects of higher frequency modes of the structure were accounted for by the inclusion of high frequency unmodeled dynamics attenuation.

The μ-framework allows for the incorporation of structured and unstructured uncertainties of the plant model into the controller design. The focus of the research efforts is on robust control for flexible structures with both unstructured and structured uncertainties due to unmodeled dynamics, actuator and sensor dynamics and uncertainties in damping, frequencies and mode shapes. In the future experiment (II), the abundance of actuators and sensors on the experiment structure will make it possible to address one of the most challenging problems in larger flexible structures, non-collocated control. (Fig. 9.)

Objectives

- Experimental validation of μ-synthesis techniques for robust control of large flexible space structures on a ground experiment.
- Conduct technology experiments to quantify performance:
  - Experiment I: Employ Hub sensors/actuators to control Boom-Dish modes.
  - Experiment II: Employ Hub& Rib sensors/actuators to control Boom-Dish & Dish modes (Non-collocation of control and measurement devices).
- Design includes structured and unstructured uncertainties to cover unmodeled dynamics, sensor and actuator dynamics, and uncertainties in damping, frequencies, and mode shapes.

Figure 9.

Robust Control Design Methodology

The general framework to be used in this study is illustrated in the diagram "GENERAL FRAMEWORK" of Figure 10. Any linear interconnection of inputs, outputs, commands, perturbations, and controller can be rearranged to match this diagram. For the purpose of analysis, the controller may be thought of as just another system component and the diagram reduces to that in the diagram "ANALYSIS." The analysis problem involves determining whether the error *e* remains in a desired set of values for given norm-bounded sets of input υ and perturbation Δ. The interconnection structure G can be partitioned so that the input-output map from υ to *e* can be expressed as the linear fractional transformation $F_u(G,\Delta)$.

Similarly, for the purpose of synthesis, the Δ can be normalized properly so that the normalizing factor can be absorbed into P. This reduces the synthesis problem as that in the diagram "SYNTHESIS." Here, the synthesis problem involves finding a stabilizing controller K such that the performance requirements are satisfied under uncertainties. The interconnection structure P can be partitioned so that the input-output map from υ' to *e*' can also be expressed as the linear fractional transformation $F_l(P,K)$. (Fig. 10.)

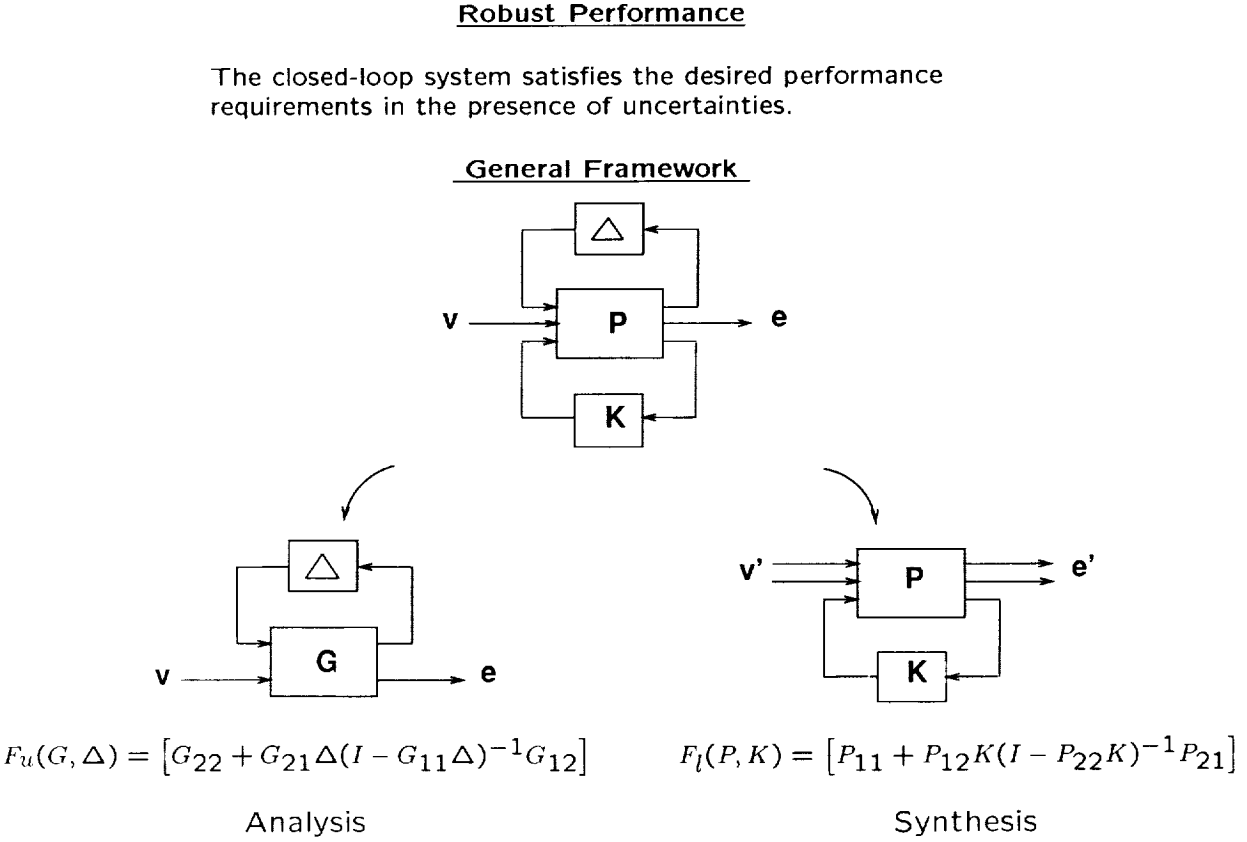

Figure 10.

Structured Singular Value Analysis
H_∞ Optimization and μ-Synthesis

The μ-synthesis methodology emerges as a practical approach in designing control systems with robust performance. This technique essentially integrates two powerful theories for synthesis and analysis into a systematic design technique that involves using the H_∞ optimization method for synthesis and the structured singular value (μ) for analysis. This technique is to find a stabilizing controller K and scaling matrix D such that the quantity

$$|| DF_l(P,K)D^{-1} ||_\infty$$

is minimized. One approach to solve this problem is to alternately minimize the above expression for either K or D while holding the other constant. For fixed D, it becomes an H_∞ optimal control problem and can be solved using the well-known state-space method. On the other hand, for fixed K, the problem can be minimized at each frequency as a convex optimization in *ln*(D). The numerical results obtained for D can be fitted with an invertible, stable, minimum-phase, real-rational transfer function. This process is carried out iteratively until a satisfactory controller is constructed. (Fig.11.)

A frequency domain method for analyzing the robustness properties of the feedback system.

$$\mu(M) = \frac{1}{\min\limits_{\Delta} \{\bar{\sigma}(\Delta) | det(I + M\Delta) = 0\}}$$

H_∞ Optimization

Find a stabilizing controller K such that

$$\|F_l(P, K)\|_\infty$$

is minimized.

μ – Synthesis

A synthesis technique to design closed-loop control system with robust performance. The technique is developed by combining H_∞ optimization method for controller synthesis with nominal performance and the structured singular value (μ) method for robust stability.

$$\min_{\mathcal{D}} \min_{K} \|DF_l(P, K)D^{-1}\|_\infty$$

Iterate on $\mathcal{D}$ and K to obtain the solution.

Figure 11.

Controller Design

The block diagram shows the problem formulation used to design controller K. It is required to scale all the output errors to 1, so that when μ is less than 1, robust performance is achieved for the plant and uncertainty description defined by the interconnection structure P.

The PLANT is a 2-input/2-output model consisting of 2 decoupled two-mode SISO subsystems. An uncertainty weighting "W_{unc}," associated with the unmodeled dynamics is included between the actuators and sensors as an additive uncertainty with weighting function of 3.5(s + 1)/(s + 50). Output uncertainty associated with the sensors is formulated as multiplicative uncertainty on the sensor outputs which is treated as a constant 16% uncertainty across the entire frequency spectrum to account for possible coefficient errors associated with the plant model.

In the controller design for K, the actuator magnitude was limited to 1.11 Nm. The actual limitation on the actuator force is ±2Nm. The discrepancy is due to the model having too high of a damping value for the second mode. This leads to a difference of approximately a factor of 2 between theoretical and experimental actuator force levels. Sensor noises, on the order of ±1 mrad, are also included in the problem formulation.

The performance specification of the closed-loop transfer function between input disturbance and output sensors is defined. The performance weight consists of a constant weighting of 2.2. This requires the peak value of the magnitude in the closed-loop transfer function between the disturbance and sensors be reduced by 2.2. A straight H_∞ control design will not be able to take advantage of the knowledge of this structure, whereas controllers formulated using μ-synthesis can, via D scalings. (Fig. 12.)

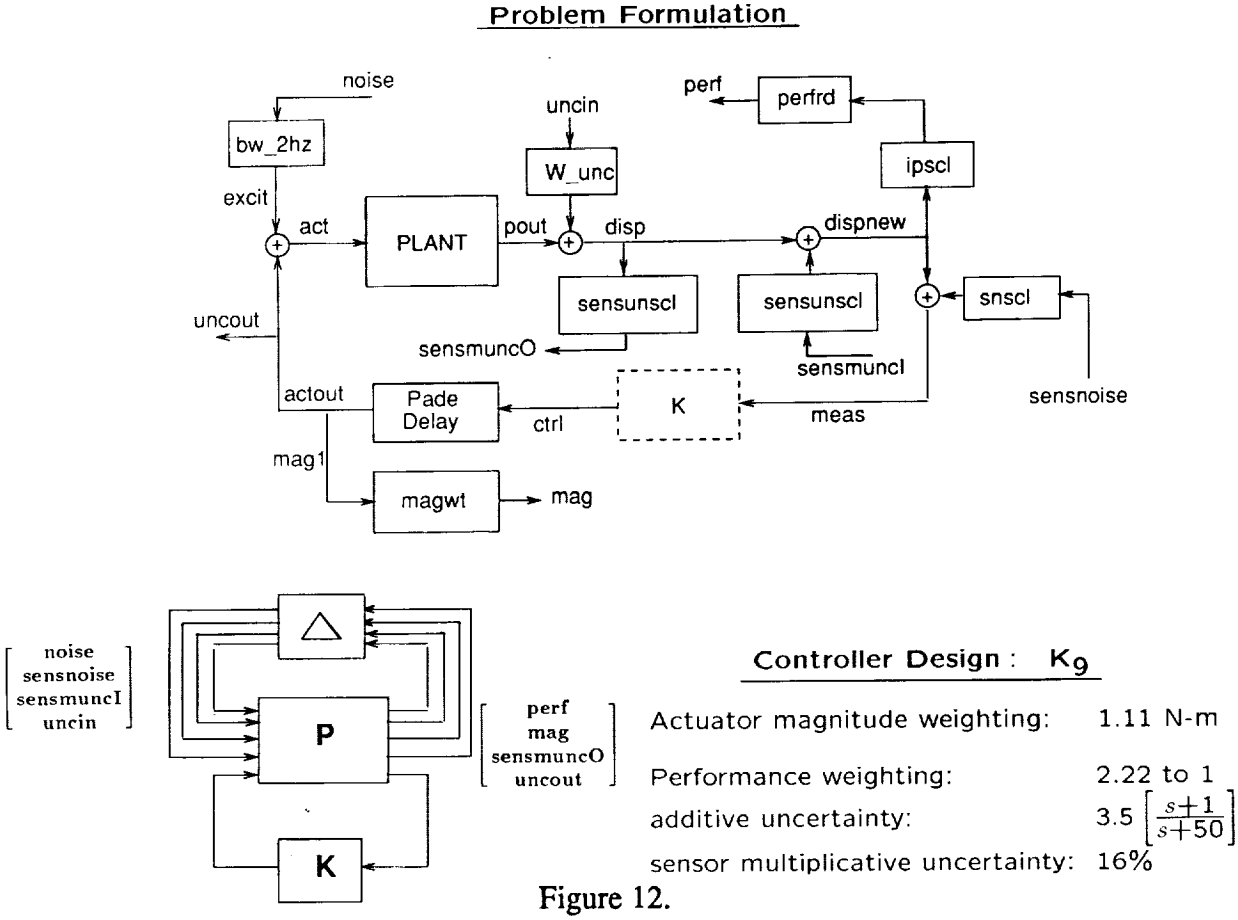

Figure 12.

Summary of Experiment Results

The unreduced controller has 16 states. Since the 2 axes are decoupled, the controller can be implemented with two independent channels where each channel is an 8th order system. To ease the computational burden, each of the 8th order systems was reduced to a 5th order system using balanced minimal realization methods. Theoretical analysis shows that the reduced order controller should have little effect on performance and robustness as compared with the full order controller.

Figure 13 shows the open-loop and closed-loop responses. The structure was first excited with 8 pulses of 0.8 second each. The force amplitude of each pulse was ± 1 Nm. The settling time was the time required for the response to drop to smaller than 2 milliradians. The closed-loop system is robust and stable. Its settling time is 4 times shorter than that of the open-loop response.

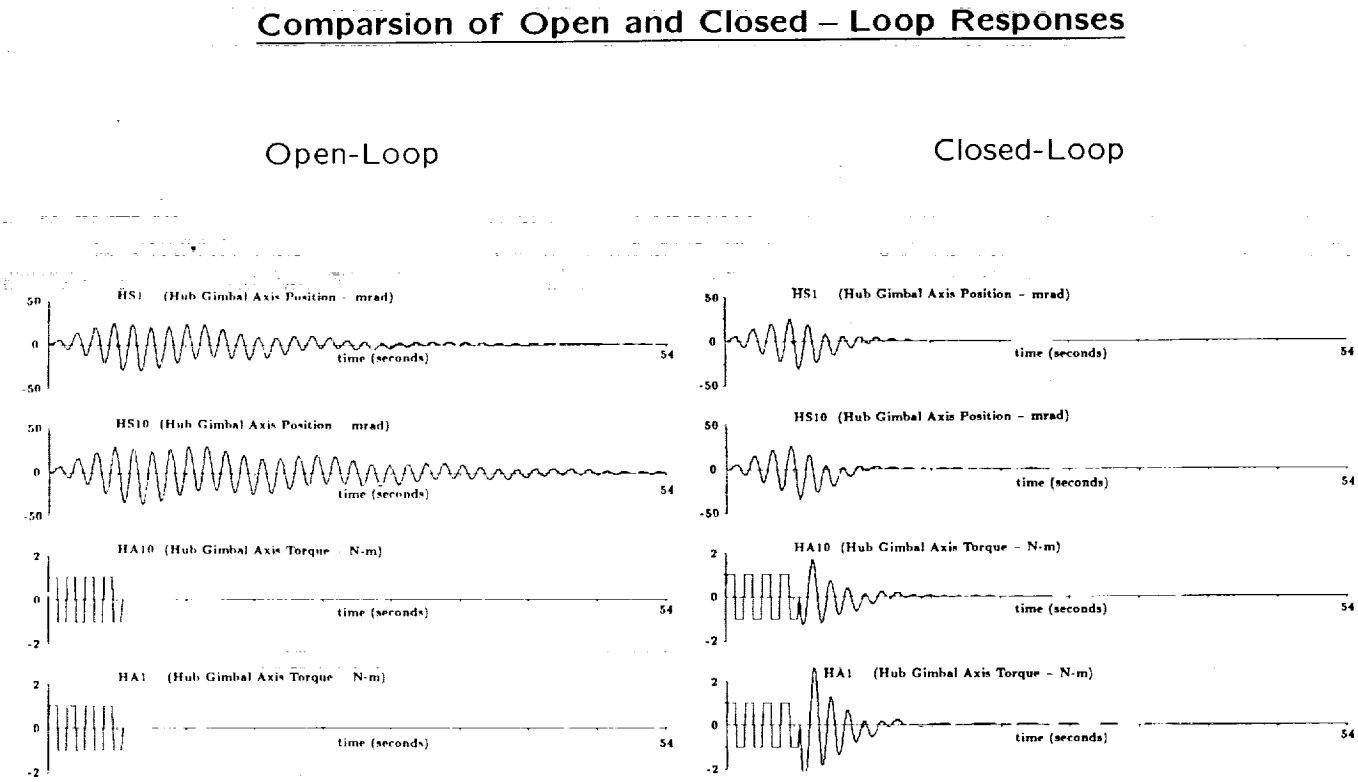

Figure 13.

Conclusions -- μ-Synthesis Experiment

Using the μ-framework, we were able to synthesize control designs which performed well on the experimental system. This control design achieves high vibration attenuation at the natural frequencies of the experiment structure. The performance of the experiment is limited by the actuator torque available. Increased actuator torque would certainly increase the performance capability of the stucture.

Future experiment work is planned. This work will include increasing the number of actuators and sensors used, and addressing the issues of non-collocated sensors and actuators. Additional sensors and actuators will allow more modes of the system to be damped and will potentially increase vibration attenuation across the frequency spectrum of the structure. Robustness issues will also be addressed. The control designs will be tested to determine their robustness to various types of uncertainties associated with the plant, actuators, and sensors. (Fig.14.)

- A robust control design using μ-synthesis was achieved which exhibited good performance on the experimental facility.
- Performance is severely compromised by the force limits in hub actuators.
- μ-synthesis provides an attractive design technique for vibration attenuation and robust control.
- Future work includes using additional sensors and actuators on the ribs to control a wide range of structural modes.

Figure 14.

System Identification Experiment
(Y. Yam, D. Bayard, F. Hadaegh, E. Mettler)

The analysis, design, and on-orbit tuning of robust controllers requires more information about the plant than simply a nominal estimate of the plant transfer function. Information is also required to characterize the uncertainty in the nominal estimate. A frequency domain identification methodology for large space structure has been developed by JPL which makes use of a simple but useful characterization of the model uncertainty based on the output error. This is a characterization of the "additive uncertainty" in the plant model, which has found considerable use in many robust control analysis and sysnthesis techniques. Experimental demonstration of the methodology via the experiment structure test bed is focused to support the objectives including: 1) to experimentally verify the performance of the system ID methodology; 2) to estimate system quantities useful for robust control analysis and redesign; 3) to demonstrate the automated operations of system identification in on-orbit scenarios; and 4) to obtain via actual dynamics a verified model of the testbed structure which will be available for analysis and controller design. (Fig. 15.)

- **OBJECTIVES**
  - **EXPERIMENTAL VERIFICATION OF THE SYSTEM ID METHODOLOGY**
  - **ESTIMATION OF SYSTEM QUANTITIES FOR ROBUST CONTROL ANALYSIS AND REDESIGN**
  - **DEMONSTRATION OF ON-ORBIT AUTOMATED SYSTEM ID SCENARIOS**
  - **DETERMINATION VIA ACTUAL DYNAMICS OF A "VERIFIED" MODEL FOR ANALYSIS/CONTROLLER DESIGN**

- **PHASE I EXPERIMENT CHARACTERISTICS**
  - **SIMO OPERATIONS**
  - **WIDEBAND, NARROWBAND, SINE-DWELL EXPERIMENTS**
  - **INSTRUMENTATION: HUB TORQUERS, HUB ANGULAR SENSORS, LEVITATOR SENSORS**
  - **BOOM-DISH MODAL EXCITATION: FREQUENCY < 10 Hz**

Figure 15.

Frequency Domain System ID Methodology

Figure 16 (shown below) summarizes the Phase I experimental verification of the identification methodology. The experiments utilized single input and multiple (usually 5) outputs. Several investigations utilizing wideband, narrowband, and sine-dwell excitations were performed. Areas of investigation included reduced order model identification, residual mode excitation and analysis, system nonlinearity, and noise anomaly. Experiments were conducted about the 1-7 and 4-10 hub axes of the test bed structure using the corresponding hub torquers for actuation. The set of sensors utilized included the hub angular sensors and some levitator sensors for characterization of the system dynamics. The sampling frequency was 20 Hz, hence only modes with frequency under 10 Hz, were under investigation. Note that the dish modes, with their symmetric mode shapes about the hub, are not controllable and observable from the hub. Thus, the phase I identification experiments investigate only the boom-dish modes via actuation at the hub. Since these modes constitute a small subset of all system modes and have larger frequency separation, they provide a good first test of the performance of the ID methodology. As experience and confidence in experimentation and algorithm performance grows, the dish modes will be tackled in phase II identification experiments.

- **ON-LINE DIGITAL FILTER/OPTIMAL INPUT DESIGN**
- **MODAL ORDER DETERMINATION USING PRODUCT MOMENT MATRIX (PMM)**
- **PLANT TRANSFER FUNCTION ESTIMATED BY CROSS-CORRELATION h=Puy/Puu**
- **PARAMETRIC MODEL CURVE FIT BASED ON h AND PMM MODAL ORDER TEST RESULTS**
- **OUTPUT ERROR/ADDITIVE UNCERTAINTY DETERMINATION FOR ROBUSTNESS ANALYSIS**

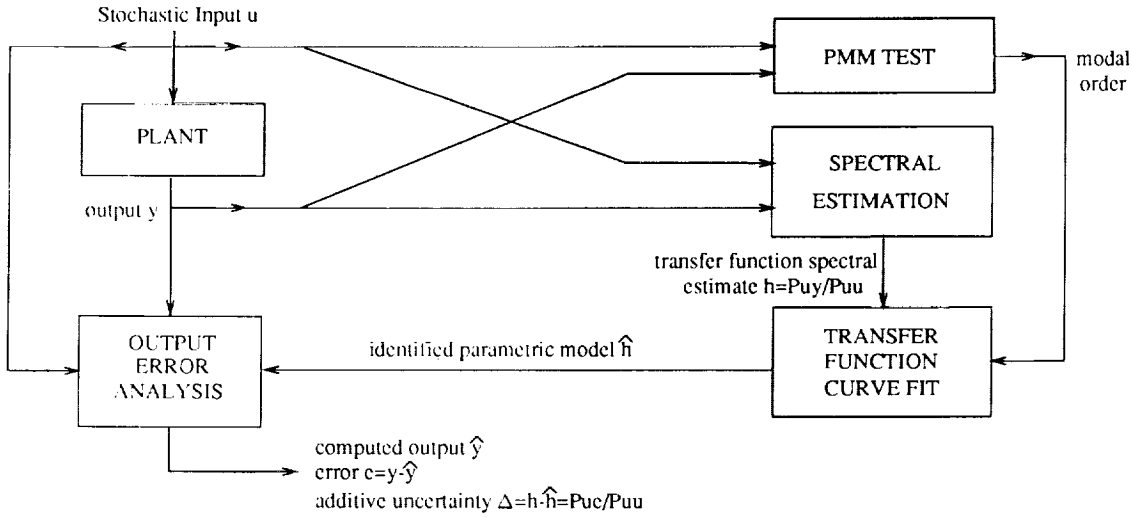

AUTOMATED FREQUENCY DOMAIN SYSTEM IDENTIFICATION METHODOLOGY

Figure 16.

Experiment Results -- The 4-10 Axis

Results of a wideband excitation experiment are shown in figures 17A to H. The experiment was performed on the 4-10 hub axis of the experiment structure utilizing the hub torquer and sensor for instrumentation. The sampling frequency was 20 Hz. The experiment run time was 1638.4 sec. Figure A shows the white noise excitation u uniformly distributed between the range ± 1.5 Nm. The output response y is shown in figure B. Figure C shows the PMM test determinant values as a function of the assumed model order. This test yielded a model order of 3 for the system. Figure D presents the transfer function spectral estimate h. Transfer function curve fitting on h was performed assuming a model order of 3, giving rise to the identified parametric model of Figure E. Both gain and phase values of h are utilized in the curve fitting. The identified frequencies and damping coefficients are 0.114 Hz, 0.637 Hz, and 2.57 Hz, and 0.4, 0.0364, and 0.00604, respectively. Figure F shows the computed output y of the identified parametric model subjected to the same excitation. Figure G shows the output error e, which has a maximum of 2.6 mrad as compared to 10 mrad for $\hat{y}$. Finally, the additive uncertainty spectral estimate Δ is shown in Figure H. It indicates the identification of the modal dynamics to within 10% to 30%. There are two modes, apparent in figure D, that were not fitted. Figure H shows that the error resulting from omitting those modes is even smaller than the fitting error of the identified modes. The curve fitting algorithm has properly determined their omission and produced a reduced-order plant model which minimizes the additive uncertainty.

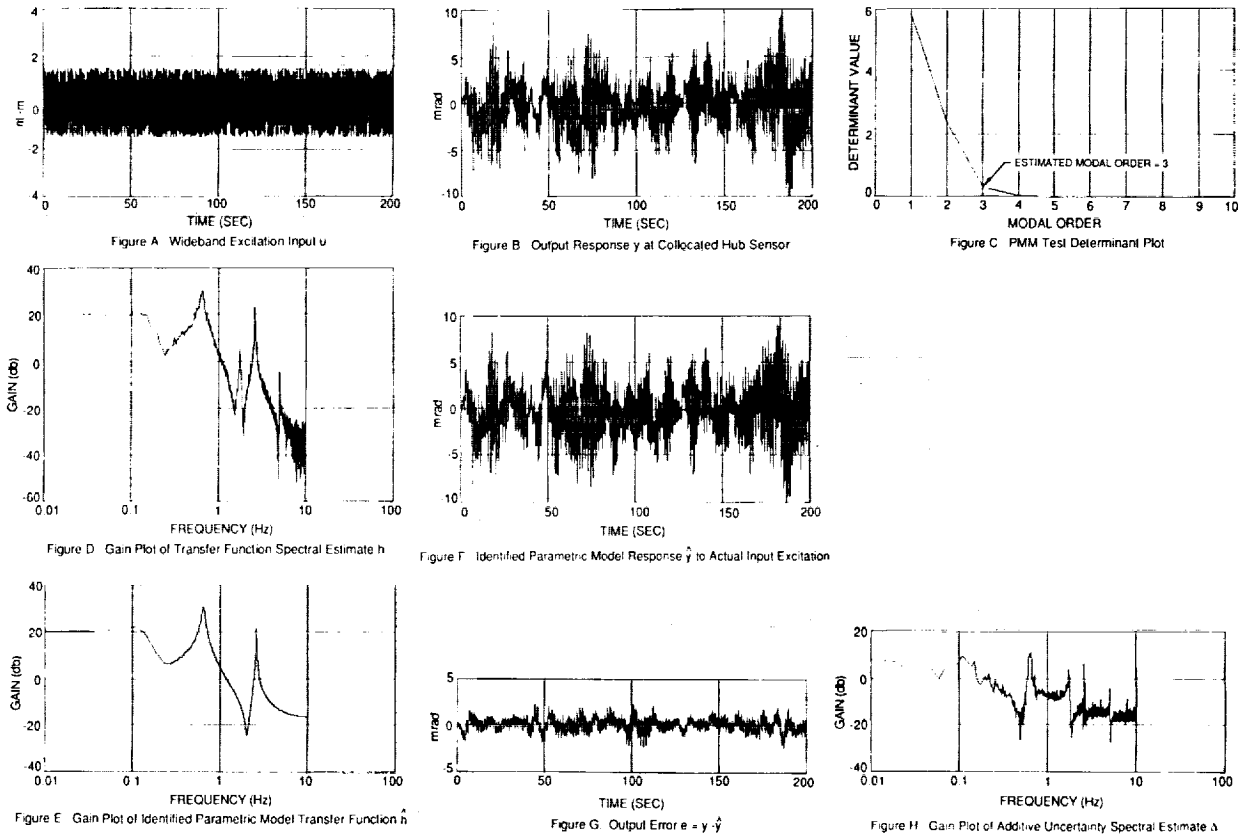

Figure 17.

Comparative Analysis and Summary

The table on the right tabulates the modal frequency values of the 1st, 2nd, and 4th modes for the two axes as determined from finite element modelling method and experiment results. The two sets of results agree exceptionally well for the 4th mode and reasonably well for the others. In general, the experimental results confirm that the 4-10 axis have slightly smaller frequency values than the 1-7 axis which was predicted analytically by the finite element model.

The high damping coefficients for mode 1 estimated by the experiment were caused by a hardware problem in the experiment facility at the time this experiment was performed which caused high damping levels. This problem was later corrected. High damping also reduces the accuaracy of the predicted modal frequencies. This may help to explain the relatively larger modal frequency. This may also explain the relatively larger frequency separation of this mode between the values predicted by the finite element model and determined from this experiment. (Fig. 18.)

(A) THE 1-7 AXIS

MODE #	FEM		EXPERIMENT	
	FREQ (Hz)	DAMPING COEF.	FREQ (Hz)	DAMPING COEF.
1	0.091	--	0.126	0.32
2	0.628	--	0.666	0.0564
4	2.682	--	2.68	0.00746

(B) THE 4-10 AXIS

MODE #	FEM		EXPERIMENT	
	FREQ (Hz)	DAMPING COEF.	FREQ (Hz)	DAMPING COEF.
1	0.091	--	0.114	0.4
2	0.616	--	0.637	0.0364
4	2.577	--	2.57	0.00604

SUMMARY

- CURVE FITTING ALGORITHM PRODUCED A GOOD REDUCED-ORDER PLANT MODEL
- IDENTIFIED MODEL AND ADDITIVE UNCERTAINTY PROVIDE CRUCIAL INFORMATION FOR ROBUST CONTROL DESIGN
- AUTOMATED SYSTEM IDENTIFICATION METHODOLOGY VERIFIED

Figure 18.

Summary and Conclusions

This paper has described the test bed developed at JPL for experimental evaluation of new technologies for the control of large flexible space structures. The experiment consists of a flexible spacecraft dynamic simulator, sensors, actuators, a microcomputer, and an advanced programming environment. The test bed has been operational for over a year, and thus far nine experiments have been completed or are currently in progress. Several of these experiments were reported at the 1987 CSI Conference, and several recent ones are documented in this paper, including high-order adaptive control, non-parametric system identification, and mu-synthesis robust control. An aggressive program of experiments is planned for the forseeable future. (Fig. 19.)

- **PROGRAM OBJECTIVE**
  - DEMONSTRATE AND VALIDATE CRITICAL CONTROL METHODOLOGIES ON A PHYSICAL STRUCTURE
- **EXPERIMENTS COMPLETED TO DATE OR IN PROGRESS**
  - UNIFIED MODELING AND CONTROL DESIGN
  - MODEL REFERENCE ADAPTIVE CONTROL (TWO INPUT/TWO OUTPUT)
  - STATIC SHAPE DETERMINATION
  - SHAPE DETERMINATION VIA COMPUTER VISION
  - SENSOR VALIDATION (SHAPES)
  - FREQUENCY DOMAIN SYSTEM IDENTIFICATION
  - HIGH-ORDER ADAPTIVE CONTROL (SIX INPUT/SIX OUTPUT)
  - MU-SYNTHESIS ROBUST CONTROL (I – DONE, II – PLANNED)
  - MODAL SURVEY (IN PROGRESS)
- **SEVERAL GI EXPERIMENTS PLANNED FOR FY'89 AND FY'90**

Figure 19.